1-1-2015

Absolute phase recovery of three fringe patterns with selected spatial frequencies

Yi Ding
Huazhong University of Science and Technology

Jiangtao Xi
University of Wollongong, jiangtao@uow.edu.au

Yanguang Yu
University of Wollongong, yanguang@uow.edu.au

Fuqin Deng
Harbin Institution Of Technology

Absolute phase recovery of three fringe patterns with selected spatial frequencies

Abstract

A new temporal approach is presented for the recovery of the absolute phase maps from their wrapped versions based on the use of fringe patterns of three different spatial frequencies. In contrast to the two-frequency method recently published, the method proposed is characterized by better anti-error capability as measured by phase error tolerance bound. A general rule for the selection of the three frequencies is presented, and its relationship to the phase error tolerance bound is derived. Theoretical analysis and experimental results are also presented to validate the effectiveness of the proposed three frequency technique.

Keywords

spatial, selected, patterns, fringe, three, recovery, phase, frequencies, absolute

Disciplines

Engineering | Science and Technology Studies

Publication Details

Y. Ding, J. Xi, Y. Yu & F. Deng, "Absolute phase recovery of three fringe patterns with selected spatial frequencies," Optics and Lasers in Engineering, vol. 70, pp. 18-25, 2015.

Absolute phase recovery of three fringe patterns with selected spatial frequencies

Yi Ding[1], Jiangtao Xi[2,*], Yanguang Yu[2], Fuqin Deng[3]

[1]*Shenzhen Institution of Advanced Technology, Chinese Academy of Science, 1068 Xueyuan Avenue, Shenzhen, 518055, China*

[2] *School of Electrical Computer and Telecommunications Engineering, University of Wollongong, Wollongong, NSW, 2522, Australia*

[3]*Shenzhen Graduate School, Harbin Institution of Technology, Shenzhen, 518055, China*

[*]*jiangtao@uow.edu.au*

Abstract: A new temporal approach is presented for the recovery of the absolute phase maps from their wrapped versions based on the use of the fringe patterns of three different spatial frequencies. In contrast to the two-frequency method recently published, the method proposed is characterized by better anti-error capability as measured by phase error tolerance bound. A general rule for the selection of the three frequencies is presented, and its relationship to the phase error tolerance bound is derived. Theoretical analysis and experimental results are also presented to validate the effectiveness of the proposed three frequency technique.

OCIS codes (Key words): (100.2650) Fringe analysis; (050.5080) Phase shift; (150.6910) Three-dimensional sensing; (100.5088) Phase unwrapping; (120.6650) Surface measurements.

1. Introduction

Fringe projection profilometry (FPP) is one of the most promising technologies for non-contact 3D shape measurement. A challenging task associated with existing phase measurement technique in FPP is phase unwrapping operation, which aims to recover the absolute phase maps from the wrapped phase maps. Existing phase unwrapping methods include spatial [1], temporal [2, 3], and period coding [4]. However, recovery of absolute phase maps is still a challenging task when the wrapped phase maps contain noise, sharp changes or discontinuities [5].

To achieve reliable and accurate phase unwrapping for FPP, a variety of temporal phase unwrapping approaches have been proposed following work of Huntley and Saldner [2]. The general idea behind this temporal method is that multiple fringe patterns are projected onto the object, yielding a sequence of wrapped phase maps as a function of time t. These phase maps can be considered as a 3D phase map $\phi(m,n,t)$, denoting the wrapped phase value at pixel (m,n) at the tth phase map ($t=0, 1, 2, \ldots, s$). Phase unwrapping can be carried out along any path in the 3D space in order to avoid noise or boundaries and thus achieving correct recovery of the absolute phase map. While the method proposed in [2] is demonstrated to be effective for accurate phase unwrapping, it also suffers from the drawback of requiring many intermediate phase patterns (e.g., 7 sets of fringe patterns were employed in [2]), which is obviously not suitable for fast or real-time measurement. In order to increase the efficiency, Zhao, *et al.* [3] propose to use two image patterns, one of which has a very low spatial frequency in contrast to the other. In particular, the low spatial frequency pattern only has a single fringe. Such a pattern has its absolute phase value falling within the range $(-\pi,\pi)$, and hence can be used as a reference to calculate the fringe number of the other fringe pattern, thus yielding its absolute phase map. Li, *et al.* [5, 6] also employ the phase map of single fringe pattern as reference to unwrap high spatial frequency fringe patterns, and it is shown that the spatial frequency of the pattern to be unwrapped is determined by the level of noise. Following the same method in [5], Liu, *et al.* [7] project a single fringe pattern and a high frequency pattern in one shot to

accelerate the speed of 3D measurement. These method works well in principle, but the gap between two spatial frequencies should be restricted within a range based on the noise level or steps in the low frequency phase maps. As the accuracy performance of FPP requires the use of high frequency fringe patterns, these methods may not work well when the phase maps are noisy or discontinuous. Consequently, multiple intermediate image patterns are still required in order to reduce the frequency gaps among adjacent patterns. Saldner and Huntley [8, 9] study the multiple intermediate image patterns, showing that to unwrap a phase map of frequency *f*, $\log_2 f + 1$ sets of fringe patterns are required. A similar result is also reached by Zhang [10, 11], indicating that the spatial frequency can be increased by a factor of 2 between two adjacent patterns. Taking a typical FPP arrangement as an example where the image pattern has 16 fringes, 5 image patterns are still required with this approach.

In order to recover the absolute phase maps of high spatial frequency fringes with less number of fringe patterns, we have developed a temporal phase unwrapping technique based on the use of two fringe images with two selected frequencies [12]. When the two normalized spatial frequencies f_1 and f_2 are coprime, there exists a one-to-one map from $[f_2\phi_1(x) - f_1\phi_2(x)]/2\pi$ to their fringe orders, where $\phi_1(x)$, $\phi_2(x)$ are the wrapped phase maps. We also obtain the minimal value gap of $[f_2\phi_1(x) - f_1\phi_2(x)]/2\pi$ when f_1 and f_2 are coprime. However, the performance of the proposed method in [12] is limited by phase error tolerance bound, $\pi/(f_1 + f_2)$ [13]. If the phase error of wrapped phase maps is larger than the phase error bound, errors may occur in the recovery of the absolute phase maps. As demonstrated by the experiments in [13], phase errors in many practical situations are significant and can easily exceed the bound, leading to the failure in recovering the absolute phase map. Therefore, it is desirable to develop new approaches with the aim to increase phase error tolerance bound. To this end, we propose a method based on the projection of three fringe patterns with selected frequencies. The idea is that with the use of three spatial fringe patterns, the minimal value gap on the values of $[f_2\phi_1(x) - f_1\phi_2(x)]/2\pi$ can be increased to higher than one, resulting in a higher phase error tolerance bound.

Zhong, *et al.* [14] also constructed a look-up table to unwrap the absolute phase maps for multiple-spatial-frequency fringes. This look-up table denotes the corresponding relationship from a pair of fringe orders at two spatial frequencies (f_1, f_2) to $[f_2\phi_1(x) - f_1\phi_2(x)]/2\pi$. When the spatial frequencies f_1 and f_2 are large values, one value in $[f_2\phi_1(x) - f_1\phi_2(x)]/2\pi$ may correspond to two or more pairs of fringe orders, thus the fringe orders can not be determined uniquely. To make sure the values of $[f_2\phi_1(x) - f_1\phi_2(x)]/2\pi$ unique, Zhong, *et al.* [15] proposed to use relatively irrational spatial frequencies for the wrapped phase maps, that is, $f_1 = 3$, $f_2 = 5$, $f_3 = 3\sqrt{2}/2$ (not the normalized spatial frequencies). To apply the relatively irrational frequencies, Zhong [16] proposed to generate the two relatively irrational spatial frequencies fringes by changing the projection angle of the grating. However, the spatial frequency selection in [14] does not guarantee the one-to-one map from $[f_2\phi_1(x) - f_1\phi_2(x)]/2\pi$ to a pair of fringe orders, thus the dynamic measurement range is smaller than the section of pattern image [15]. Furthermore, the minimal value gap of $[f_2\phi_1(x) - f_1\phi_2(x)]/2\pi$ of two irrational frequencies is always smaller than the two rational frequencies [14, 15, 16], which may yield mistakes in determining fringe order pairs. Our proposed method could guarantee the one-to-one map and increase the minimal value gap of $[f_j\phi_i(x) - f_i\phi_j(x)]/2\pi$ significantly to enhance the reliability of absolute phase maps.

This paper is organized as follows. In Section 2 we present the technique to recover the absolute phase maps with three selected frequency fringe patterns. In Section 3, we give the principle to increase the smallest value gap by selecting frequencies. In Section 4, experiments are presented to validate the effectiveness of three frequency technique and the principle to increase the value gap. Section 5 concludes the whole paper.

2. Absolute phase maps recovery with three frequency fringe patterns

2.1 Three frequency technique

Let us consider a FPP system, with which three image patterns are projected onto the object surface respectively. The image patterns are characterized by fringe structure where the light intensity is constant in y-axis and varies sinusoidally in x-axis. The normalized spatial frequencies of the three patterns are f_1, f_2 and f_3, referring to the total number of fringes on the respective patterns. Let us use $\Phi_i(x)$ (i=1,2,3) and $\phi_i(x)$ (i=1,2,3) to denote respectively the absolute phase maps and the corresponding wrapped phase maps of the fringe patterns. Taking the central vertical line of images as the reference, the value of the wrapped phase map is limited by $-\pi \le \phi_i(x) \le \pi$ (i=1,2,3), and the value of the absolute phase maps should fall into the following:

$$-f_1\pi \le \Phi_1(x) \le f_1\pi\ ,\ \ -f_2\pi \le \Phi_2(x) \le f_2\pi\ ,\ \ -f_3\pi < \Phi_3(x) < f_3\pi \tag{1}$$

Hence the absolute and wrapped phase maps are related by the following:

$$\Phi_i(x) = 2\pi m_i(x) + \phi_i(x) \tag{2}$$

Where $m_i(x)$ (i=1,2,3) are referred to as fringe numbers or indices. They are integers and $-\lfloor f_i/2 \rfloor < m_i(x) < \lfloor f_i/2 \rfloor$ (i=1,2,3). Obviously, the absolute phases can be recovered if $m_i(x)$ (i=1,2,3) are determined. In order to achieve this, we employ the following relationships [10]:

$$f_2\Phi_1(x) = f_1\Phi_2(x)\ ,\ \ f_3\Phi_1(x) = f_1\Phi_3(x) \tag{3}$$

Combining Equations (2) and (3), we have:

$$\frac{f_2\phi_1(x) - f_1\phi_2(x)}{2\pi} = m_2(x)f_1 - m_1(x)f_2\ ,\ \ \frac{f_3\phi_1(x) - f_1\phi_3(x)}{2\pi} = m_3(x)f_1 - m_1(x)f_3 \tag{4}$$

Similar to the method employed in [12, 13], an intermediate variable $\Phi_0(x)$ is introduced, which increases monotonically from $-\pi$ to π with respect to x and defined as follows:

$$\Phi_0(x) = \frac{\Phi_1(x)}{f_1} = \frac{\Phi_2(x)}{f_2} = \frac{\Phi_3(x)}{f_3} \tag{5}$$

Considering $\Phi_0(x) = \Phi_1(x)/f_1$ and taking account of Equation (1), $m_i(x)$ (i=1,2,3) can be determined by the value of $\Phi_0(x)$ as follows:

$$m_1(x) = \begin{cases} \lfloor f_1/2 \rfloor & [f_1 - (f_1 \bmod 2 + 1)]\pi/f_1 \le \Phi_0(x) < \pi \\ \quad\cdots & \quad\cdots \\ \quad 1 & \quad \pi/f_1 \le \Phi_0(x) < 3\pi/f_1 \\ \quad 0 & \quad -\pi/f_1 < \Phi_0(x) < \pi/f_1 \\ \quad -1 & \quad -3\pi/f_1 \le \Phi_0(x) < -\pi/f_1 \\ \quad\cdots & \quad\cdots \\ -\lfloor f_1/2 \rfloor & -\pi < \Phi_0(x) \le -[f_1 - (f_1 \bmod 2 + 1)]\pi/f_1 \end{cases} \tag{6}$$

$$m_2(x) = \begin{cases} \lfloor f_2/2 \rfloor & [f_2 - (f_2 \bmod 2 + 1)]\pi/f_2 \le \Phi_0(x) < \pi \\ \quad\cdots & \quad\cdots \\ \quad 1 & \quad \pi/f_2 \le \Phi_0(x) < 3\pi/f_2 \\ \quad 0 & \quad -\pi/f_2 < \Phi_0(x) < \pi/f_2 \\ \quad -1 & \quad -3\pi/f_2 < \Phi_0(x) \le -\pi/f_2 \\ \quad\cdots & \quad\cdots \\ -\lfloor f_2/2 \rfloor & -\pi < \Phi_0(x) \le -[f_2 - (f_2 \bmod 2 + 1)]\pi/f_2 \end{cases} \tag{7}$$

$$m_3(x)=\begin{cases} \lfloor f_3/2 \rfloor & [f_3-(f_3 \bmod 2+1)]\pi/f_3 \le \Phi_0(x) < \pi \\ \quad\cdots & \quad\cdots \\ 1 & \pi/f_3 \le \Phi_0(x) < 3\pi/f_3 \\ 0 & -\pi/f_3 < \Phi_0(x) < \pi/f_3 \\ -1 & -3\pi/f_3 < \Phi_0(x) \le -\pi/f_3 \\ \quad\cdots & \quad\cdots \\ -\lfloor f_3/2 \rfloor & -\pi < \Phi_0(x) \le -[f_3-(f_3 \bmod 2+1)]\pi/f_3 \end{cases} \tag{8}$$

where $\lfloor x \rfloor$ denotes the operation of taking the largest integer not greater than x.

Equations (6-8) give a unique mapping from $\Phi_0(x)$ to $m_i(x)$ (i=1,2,3), implying that $\Phi_0(x)$ can be employed to determine $m_i(x)$ (i=1,2,3), but $\Phi_0(x)$ is not available. However, combining the right hand side of Equations (6-8) we can see that the value of $\Phi_0(x)$ can be divided into many small intervals, each of which corresponds to particular set of $m_i(x)$ (i=1,2,3). Then if there is an unique mapping from $m_1(x)f_3 - m_3(x)f_1$ and $m_3(x)f_2 - m_2(x)f_3$ to the intervals, we can establish a mapping relationship from $[f_3\phi_1(x) - f_1\phi_3(x)]/2\pi$ and $[f_3\phi_2(x) - f_2\phi_3(x)]/2\pi$ to $m_i(x)$ (i=1,2,3), and the relationship can be used to determine the latter. In order to illustrate the effectiveness of such an idea, let us consider an example where $f_1 = 6$, $f_2 = 10$ and $f_3 = 15$. From Equations (6-8) we can derive the following relationship in Table 1. The first column in Table 1 gives the intervals of $\Phi_0(x)$, covering the whole range $-\pi < \Phi_0(x) < \pi$. The second column shows the values of $m_i(x)$ (i=1,2,3) corresponding to each of the intervals, and the third and fourth column give the corresponding values of $[f_3\phi_1(x) - f_1\phi_3(x)]/2\pi$ and $[f_3\phi_2(x) - f_2\phi_3(x)]/2\pi$. It is seen that each row on the table gives a mapping from $[f_3\phi_1(x) - f_1\phi_3(x)]/2\pi$ and $[f_3\phi_2(x) - f_2\phi_3(x)]/2\pi$ to $m_i(x)$ (i=1,2,3), which is different from others and hence unique. Therefore, if a pair of $[f_3\phi_1(x) - f_1\phi_3(x)]/2\pi$ (that is, $m_1(x)f_3 - m_3(x)f_1$) and $[f_3\phi_2(x) - f_2\phi_3(x)]/2\pi$ (that is, $m_3(x)f_2 - m_2(x)f_3$) is known, we can use the second, the third and the fourth column of Table 1 to determine the values of $m_i(x)$ (i=1,2,3).

Table 1 Mapping from $\Phi_0(x)$ to ($m_1(x)$, $m_2(x)$, $m_3(x)$) and ($[f_3\phi_1(x) - f_1\phi_3(x)]/2\pi$, $[f_2\phi_1(x) - f_1\phi_2(x)]/2\pi$)

$\Phi_0(x)$	$m_1(x), m_2(x), m_3(x)$	$\frac{f_3\phi_1(x) - f_1\phi_3(x)}{2\pi}$	$\frac{f_2\phi_1(x) - f_1\phi_2(x)}{2\pi}$
$9\pi/10 \le \Phi_0(x) < \pi$	3,5,7	-3	0
$13\pi/15 \le \Phi_0(x) < 9\pi/10$	3,4,7	-3	-6
$5\pi/6 \le \Phi_0(x) < 13\pi/15$	3,4,6	-9	-6
$11\pi/15 \le \Phi_0(x) < 5\pi/6$	2,4,6	6	4
$7\pi/10 \le \Phi_0(x) < 11\pi/15$	2,4,5	0	4
$9\pi/15 \le \Phi_0(x) < 7\pi/10$	2,3,5	0	-2
$\pi/2 \le \Phi_0(x) < 9\pi/15$	2,3,4	-6	-2
$7\pi/15 \le \Phi_0(x) < \pi/2$	1,2,4	9	2
$5\pi/15 \le \Phi_0(x) < 7\pi/15$	1,2,3	3	2
$3\pi/10 \le \Phi_0(x) < 5\pi/15$	1,2,2	-3	2
$3\pi/15 \le \Phi_0(x) < 3\pi/10$	1,1,2	-3	-4
$\pi/6 \le \Phi_0(x) < 3\pi/15$	1,1,1	-9	-4

$\pi/10 \le \Phi_0(x) < \pi/6$	0,1,1	6	6
$\pi/15 \le \Phi_0(x) < \pi/10$	0,0,1	6	0
$-\pi/15 < \Phi_0(x) < \pi/15$	0,0,0	0	0
$-\pi/10 < \Phi_0(x) \le -\pi/15$	0,0,-1	-6	0
$-\pi/6 < \Phi_0(x) \le -\pi/10$	0,-1,-1	-6	-6
$-3\pi/15 < \Phi_0(x) \le -\pi/6$	-1,-1,-1	9	4
$-3\pi/10 < \Phi_0(x) \le -3\pi/15$	-1,-1,-2	3	4
$-5\pi/15 < \Phi_0(x) \le -3\pi/10$	-1,-2,-2	3	-2
$-7\pi/15 < \Phi_0(x) \le -5\pi/15$	-1,-2,-3	-3	-2
$-\pi/2 < \Phi_0(x) \le -7\pi/15$	-1,-2,-4	-9	-2
$-9\pi/15 < \Phi_0(x) \le -\pi/2$	-2,-3,-4	6	2
$-7\pi/10 < \Phi_0(x) \le -9\pi/15$	-2,-3,-5	0	2
$-11\pi/15 < \Phi_0(x) \le -7\pi/10$	-2,-4,-5	0	-4
$-5\pi/6 < \Phi_0(x) \le -11\pi/15$	-2,-4,-6	-6	-4
$-13\pi/15 < \Phi_0(x) \le -5\pi/6$	-3,-4,-6	9	6
$-9\pi/10 < \Phi_0(x) \le -13\pi/15$	-3,-4,-7	3	6
$-\pi < \Phi_0(x) \le -9\pi/10$	-3,-5,-7	3	0

With the above we can reconstruct the absolute phase maps of three fringe patterns by the following steps:

1. Select three frequencies (f_1, f_2, f_3) and construct a table similar to Table 1, making sure the table provides a unique mapping from a pair of $[f_3\phi_1(x) - f_1\phi_3(x)]/2\pi$ ($m_1(x)f_3 - m_3(x)f_1$) and $[f_3\phi_2(x) - f_2\phi_3(x)]/2\pi$ ($m_3(x)f_2 - m_2(x)f_3$) to $m_i(x)$ (i=1,2,3) ;
2. Project onto the object with three fringe patterns of spatial frequencies (f_1, f_2, f_3) respectively, acquiring three wrapped phase maps by a phase detection algorithm;
3. Calculate the terms $[f_3\phi_1(x) - f_1\phi_3(x)]/2\pi$ and $[f_3\phi_2(x) - f_2\phi_3(x)]/2\pi$, round their values into the closest integers, denoted as *M1* and *M2*. Look up the table constructed in Step 1, find the row (or entry) whose values of $[f_3\phi_1(x) - f_1\phi_3(x)]/2\pi$ and $[f_3\phi_2(x) - f_2\phi_3(x)]/2\pi$ are the closest to *M1* and *M2*. Record the corresponding $m_i(x)$ (i=1,2,3) in the same row; Reconstruct the absolute phase maps by Equation (2) using $m_i(x)$ (i=1,2,3).

2.2 Selection of the three spatial frequencies

The validity of the approach proposed in 2.1 relies on the existence of unique mapping from a pair ($[f_3\phi_1(x) - f_1\phi_3(x)]/2\pi$, $[f_3\phi_2(x) - f_2\phi_3(x)]/2\pi$) to a combination ($m_1(x)$, $m_2(x)$, $m_3(x)$). That is, f_1, f_2, f_3 must be selected so that such a unique mapping relation is held.

In order to achieve the above, let us look at the relationship between $\Phi_0(x)$ and $(m_1(x), m_2(x), m_3(x))$ first. From Equation (6), the range of $\Phi_0(x)$ can be divided into $N_1 = 2\lfloor f_1/2 \rfloor + 1$ intervals, and the values of $\Phi_0(x)$ on the interval boundaries are $(2n_1+1)\pi / f_1$ where $-\lfloor f_1/2 \rfloor < n_1 < \lfloor f_1/2 \rfloor$. On each of these intervals $m_1(x)$ takes a different value. Similarly, Equation (7) shows the range of $\Phi_0(x)$ can be divided into $N_2 = 2\lfloor f_2/2 \rfloor + 1$ intervals, and the

values of $\Phi_0(x)$ on the interval boundaries are $(2n_2+1)\pi / f_2$ where $-\lfloor f_2/2 \rfloor < n_2 < \lfloor f_2/2 \rfloor$. On each of these intervals $m_2(x)$ takes a different value. Similarly, Equation (8) shows the range of $\Phi_0(x)$ can be divided into $N_3 = 2\lfloor f_3/2 \rfloor + 1$ intervals, and the values of $\Phi_0(x)$ on the interval boundaries are $(2n_3+1)\pi / f_3$ where $-\lfloor f_3/2 \rfloor < n_3 < \lfloor f_3/2 \rfloor$, and on each of the intervals $m_3(x)$ takes a different value.

When f_1, f_2 and f_3 do not have the common factor other than 1, it is easy to show that boundaries of the three different intervals described above can divide the range of $\Phi_0(x)$ into several intervals, and each of the intervals must correspond to an unique combination of $(m_1(x), m_2(x), m_3(x))$. As $\Phi_0(x)$ varies from $-\pi$ to π monotonically, these intervals on $\Phi_0(x)$ will correspond to the same number of intervals on x, denoted by $\Omega_1, \Omega_2, ..., \Omega_N$. Obviously, each of $\Omega_1, \Omega_2, ..., \Omega_N$ will also correspond to a unique combination $(m_1(x), m_2(x), m_3(x))$. In summary of the above, we have the following:

Statement 1: If f_1, f_2 and *f_3 do not have the common factor other than 1, the three phase maps can be divided into strips by the intervals $x \subset [\Omega_1, \Omega_2, ..., \Omega_N]$. Each of the strips on the phase maps corresponds to a unique combination $(m_1(x), m_2(x), m_3(x))$, which can be used to recover the absolute phases.*

The above statement shows that when f_1, f_2 are f_3 do not have a common factor larger than 1, there exists a unique solution for the phase unwrapping problem. In order to show that the proposed approach in 2.1 is sufficient, we should have the following:

Statement 2: When f_1, f_2, f_3 do not have the common factor larger than 1, for any two different intervals $x_a \subset \Omega_p$, $x_b \subset \Omega_q$ and $p \neq q$, we must have two corresponding combinations of $(m_1(x), m_2(x), m_3(x))$ based on Statement 1, which also meet the following:

$$\frac{f_2\phi_1(x_a) - f_1\phi_2(x_a)}{2\pi} \neq \frac{f_2\phi_1(x_b) - f_1\phi_2(x_b)}{2\pi} \text{ or/and } \frac{f_3\phi_1(x_a) - f_1\phi_3(x_a)}{2\pi} \neq \frac{f_3\phi_1(x_b) - f_1\phi_3(x_b)}{2\pi} \quad (9)$$

The above are equivalent to the following:

$$m_2(x_a)f_1 - m_1(x_a)f_2 \neq m_2(x_b)f_1 - m_1(x_b)f_2 \text{ or/and } m_3(x_a)f_1 - m_1(x_a)f_3 \neq m_3(x_b)f_1 - m_1(x_b)f_3$$

In other words, there exists a unique mapping from $(m_1(x), m_2(x), m_3(x))$ to a pair of $(\frac{f_2\phi_1(x) - f_1\phi_2(x)}{2\pi}, \frac{f_3\phi_1(x) - f_1\phi_3(x)}{2\pi})$, or a unique mapping from $(m_1(x), m_2(x), m_3(x))$ to a pair of $(m_2(x)f_1 - m_1(x)f_2, m_3(x)f_1 - m_1(x)f_3)$.

Statement 2 is a mathematical statement which indicates that every combination of $(m_1(x), m_2(x), m_3(x))$ corresponds to a unique $(m_2(x)f_1 - m_1(x)f_2, m_3(x)f_1 - m_1(x)f_3)$. However, it is difficult to give all the possible combinations of $(m_1(x), m_2(x), m_3(x))$ to proof Statement 2.

To validate the statement 2, we employ reductio ad absurdum. There are three possible scenarios making the two combinations of $(m_1(x), m_2(x), m_3(x))$ different: (a) all of the three are different, that is $m_1(x_a) \neq m_1(x_b)$, $m_2(x_a) \neq m_2(x_b)$ and $m_3(x_a) \neq m_3(x_b)$, (b) two of the three are different (such as $m_1(x_a) = m_1(x_b)$, $m_2(x_a) \neq m_2(x_b)$ and $m_3(x_a) \neq m_3(x_b)$), (c) one of the three is different (such as $m_1(x_a) = m_1(x_b)$, $m_2(x_a) = m_2(x_b)$ and $m_3(x_a) \neq m_3(x_b)$). Without loss of generality let us discuss the first case where $m_1(x_a) \neq m_1(x_b)$, $m_2(x_a) \neq m_2(x_b)$ and $m_3(x_a) \neq m_3(x_b)$. Assume that the following is valid:

$$m_2(x_a)f_1 - m_1(x_a)f_2 = m_2(x_b)f_1 - m_1(x_b)f_2, \; m_3(x_a)f_1 - m_1(x_a)f_3 = m_3(x_b)f_1 - m_1(x_b)f_3 \quad (10)$$

Equation (11) can be rewritten as:

$$\frac{m_1(x_a)-m_1(x_b)}{f_1}=\frac{m_2(x_a)-m_2(x_b)}{f_2}=\frac{m_3(x_a)-m_3(x_b)}{f_3} \tag{11}$$

As f_1, f_2, f_3 do not have the common factor larger than 1, Equation (12) must be equivalent to the following:

$$m_1(x_a)-m_1(x_b)=kf_1,\ m_2(x_a)-m_2(x_b)=kf_2,\ m_3(x_a)-m_3(x_b)=kf_3 \tag{12}$$

where k is an integer and $k\neq 0$.

Considering the ranges of $m_1(x)$, $m_2(x)$, $m_3(x)$ given above, we have:

$$-2\left\lfloor\frac{f_1}{2}\right\rfloor\le m_1(x_a)-m_1(x_b)\le 2\left\lfloor\frac{f_1}{2}\right\rfloor,\ -2\left\lfloor\frac{f_2}{2}\right\rfloor\le m_2(x_a)-m_2(x_b)\le 2\left\lfloor\frac{f_2}{2}\right\rfloor,$$
$$-2\left\lfloor\frac{f_3}{2}\right\rfloor\le m_3(x_a)-m_3(x_b)\le 2\left\lfloor\frac{f_3}{2}\right\rfloor \tag{13}$$

Comparing Equation (12) with Equation (13), it is obvious that $k=\pm 1$. Hence we have

$$m_1(x_a)-m_1(x_b)=\pm f_1,\ m_2(x_a)-m_2(x_b)=\pm f_2,\ m_3(x_a)-m_3(x_b)=\pm f_3 \tag{14}$$

Looking at Equation (13) again, when Equation (14) is held, we must have:

$$\left\lfloor\frac{f_1}{2}\right\rfloor=\frac{f_1}{2},\ \left\lfloor\frac{f_2}{2}\right\rfloor=\frac{f_2}{2},\ \left\lfloor\frac{f_3}{2}\right\rfloor=\frac{f_3}{2} \tag{15}$$

Equation (15) implies that f_1, f_2 and f_3 are all even numbers, which is contradict to the fact that f_1, f_2 and f_3 do not have the common factor larger than 1. Hence Equation (10) will not be true for the case (a) $m_1(x_a)\neq m_1(x_b)$, $m_2(x_a)\neq m_2(x_b)$ and $m_3(x_a)\neq m_3(x_b)$, thus we have the following:

$$m_2(x_a)f_1-m_1(x_a)f_2\neq m_2(x_b)f_1-m_1(x_b)f_2 \text{ or/and } m_3(x_a)f_1-m_1(x_a)f_3\neq m_3(x_b)f_1-m_1(x_b)f_3 \tag{16}$$

Similarly, we can also show that Statement 2 is true for the cases (b) and (c). Combining Statement 1 and 2, we are able to propose the following for selection of the three spatial frequencies for the technique proposed in 2.1.

Statement 3: If f_1, f_2 and f_3 do not have the common factor larger than 1, there existing a unique mapping from ($[f_2\phi_1(x)-f_1\phi_2(x)]/2\pi$, $[f_3\phi_1(x)-f_1\phi_3(x)]/2\pi$) to ($m_1(x)$, $m_2(x)$, $m_3(x)$), which enable us to determine ($m_1(x)$, $m_2(x)$, $m_3(x)$).

Statement 3 presents a rule for the selection of the three frequencies. In contrast to the two-frequency method proposed in [13], where the two frequencies must be co-prime to each other, Statement 3 does not require that all the three frequencies are co-prime to each other, hence allows more flexibility in the selection of their values. As seen below in Section 3, this will provide advantages in terms of the anti-error capability.

3. The phase error tolerance bound

In this section we will study the performance of the proposed technique in terms of its anti-error capability. The anti-error capability of the proposed technique depends on the gaps between any two possible values of $[f_3\phi_1(x)-f_1\phi_3(x)]/2\pi$ and $[f_2\phi_1(x)-f_1\phi_2(x)]/2\pi$. The larger the gap, the more unlikely the error will occur due to the rounding operation. Hence we need to find out the smallest gaps, and we should also work out the relationship between the phase error in ($\phi_1(x)$, $\phi_2(x)$) and the smallest gap. In the example shown in Table 1, the smallest value gaps for the entries in columns three ($[f_2\phi_1(x)-f_1\phi_2(x)]/2\pi$, $f_1=6$, $f_3=15$) and column four ($[f_2\phi_1(x)-f_1\phi_2(x)]/2\pi$, $f_1=6$, $f_2=10$) are 3 and 2 respectively. In contrast to the two-frequency approach presented in [13] where the minimal gap is 1, the proposed method is obviously better in terms of its anti-error capabilities.

In order to work out the smallest gap mentioned above, let us have a look of the example in Table 1 again. It is observed that the minimal gap between the entries of $[f_3\phi_1(x)-f_1\phi_3(x)]/2\pi$ is 3, which is the common factor of the two frequencies 6 and 15; the minimal gap between the entries of $[f_2\phi_1(x)-f_1\phi_2(x)]/2\pi$ is 2, also the common factor of the two frequencies 6 and 10.

This implies that the minimal gap might equal the common factor of the two frequencies. In order to prove such a hypothesis, let us consider two fringe patterns with frequencies f_1 and f_2. When f_1 and f_2 have a common factor t *(t>1)*, the $-f_1/t$ -th (and also f_1/t -th) boundaries for $\Phi_0(x)$ defined by Equations (6) are $-\pi/t$ and π/t, will coincide to the $-f_2/t$ -th (and also f_2/t -th) boundaries defined by Equation (7), respectively. This relationship also holds for all the integer multiples of f_1/t and f_2/t. Considering the range $\Phi_0(x) \subset (-\pi/t, \pi/t)$, from Equations (6) and (7) we have

$$m_1(x) = \begin{cases} \left\lfloor \frac{f_1}{2t} \right\rfloor & [\frac{f_1}{t} - (\frac{f_1}{t} \bmod 2 + 1)]\pi \cdot \frac{1}{f_1} \le \Phi_0(x) < \frac{\pi}{t} \\ \ldots & \ldots \\ 1 & \frac{\pi}{f_1} \le \Phi_0(x) < \frac{3\pi}{f_1} \\ 0 & -\frac{\pi}{f_1} < \Phi_0(x) < \frac{\pi}{f_1} \\ -1 & -\frac{3\pi}{f_1} < \Phi_0(x) \le -\frac{\pi}{f_1} \\ \ldots & \ldots \\ -\left\lfloor \frac{f_1}{2t} \right\rfloor & -\frac{\pi}{t} < \Phi_0(x) \le -[\frac{f_1}{t} - (\frac{f_1}{t} \bmod 2 + 1)]\pi \cdot \frac{1}{f_1} \end{cases} \tag{17}$$

$$m_2(x) = \begin{cases} \left\lfloor \frac{f_2}{2t} \right\rfloor & [\frac{f_2}{t} - (\frac{f_2}{t} \bmod 2 + 1)]\pi \cdot \frac{1}{f_2} \le \Phi_0(x) < \frac{\pi}{t} \\ \ldots & \ldots \\ 1 & \frac{\pi}{f_2} \le \Phi_0(x) < \frac{3\pi}{f_2} \\ 0 & -\frac{\pi}{f_2} < \Phi_0(x) < \frac{\pi}{f_2} \\ -1 & -\frac{3\pi}{f_2} < \Phi_0(x) \le -\frac{\pi}{f_2} \\ \ldots & \ldots \\ -\left\lfloor \frac{f_2}{2t} \right\rfloor & -\frac{\pi}{t} < \Phi_0(x) \le -[\frac{f_2}{t} - (\frac{f_2}{t} \bmod 2 + 1)]\pi \cdot \frac{1}{f_2} \end{cases} \tag{18}$$

Now we look at the values of $m_2(x) f_1 - m_1(x) f_2$ over the range of $\Phi_0(x) \subset (-\pi/t, \pi/t)$. As the two frequencies have a common factor t, we have

$$m_2(x) f_1 - m_1(x) f_2 = t[m_2(x)\frac{f_1}{t} - m_1(x)\frac{f_2}{t}] \tag{19}$$

Giving t the largest common factor of the two frequencies, f_1/t and f_2/t will be coprime to each other. Also for $\Phi_0(x) \subset (-\pi/t, \pi/t)$, $m_1(x)$ and $m_2(x)$ are given by Equations (17) and (18), falling into the range $(-\lfloor f_1/2t \rfloor, \lfloor f_1/2t \rfloor)$ and $(-\lfloor f_2/2t \rfloor, \lfloor f_2/2t \rfloor)$ respectively. Hence the term $[m_2(x) f_1/t - m_1(x) f_2/t]$ is exactly the same for the same of two frequencies f_1/t and f_2/t which are co-prime to each other. From the analysis in [13] we know that the minimal gap between the vales of $[m_2(x) f_1/t - m_1(x) f_2/t]$ is 1. Obviously, the minimal gap between the vales $[m_2(x) f_1/t - m_1(x) f_2/t]$ is *t*.

Now we consider the value of $m_2(x)f_1 - m_1(x)f_2$ beyond the range $\Phi_0(x) \subset (-\pi/t, \pi/t)$. Without loss of generality, let us consider the range $\Phi_0(x) \subset [\pi/t, 3\pi/t)$. Given the values of $m_1(x)$ and $m_2(x)$ over the range $\Phi_0(x) \subset (-\pi/t, \pi/t)$, we have the following:

$$[m_1(x)]_{\Phi_0(x)\subset[\pi/t,3\pi/t)} = \frac{f_1}{t} + [m_1(x)]_{\Phi_0(x)\subset[-\pi/t,\pi/t)}, [m_2(x)]_{\Phi_0(x)\subset[\pi/t,3\pi/t)} = \frac{f_2}{t} + [m_2(x)]_{\Phi_0(x)\subset[-\pi/t,\pi/t)} \tag{20}$$

Hence we have

$$\begin{aligned}[f_1 m_2(x) - f_2 m_1(x)]_{\Phi_0(x)\subset[\pi/t,3\pi/t)} &= \left[\frac{f_1 f_2}{t} + m_2(x) - \frac{f_1 f_2}{t} - m_1(x)\right]_{\Phi_0(x)\subset[-\pi/t,\pi/t)} \\ &= [f_1 m_2(x) - f_2 m_1(x)]_{\Phi_0(x)\subset[-\pi/t,\pi/t)}\end{aligned} \tag{21}$$

Therefore values of $m_2(x)f_1 - m_1(x)f_2$ on $\Phi_0(x) \subset [\pi/t, 3\pi/t)$ is the periodic extension of its value on $\Phi_0(x) \subset (-\pi/t, \pi/t)$. In the same way we can show that $m_2(x)f_1 - m_1(x)f_2$ exhibits the same values over all the periodic extension of $\Phi_0(x) \subset (-\pi/t, \pi/t)$. Hence we have the following:

Statement 4: The minimal value gap of the elements in $m_2(x)f_1 - m_1(x)f_2$ equals to the largest common factor of the two frequencies f_1 and f_2.

Based on Statement 3 and Statement 4, we have the method to increase the minimal value gap for three frequency technique. That is, the three frequencies must not have a common factor larger than 1, but the two frequency pairs should be selected in the way to have a common factor as large as possible. For example, for three frequencies (10, 12, 15), we can formulate (10, 15) and (12, 15) two combinations. For three frequencies (8, 12, 15), we can formulate (8, 12) and (12, 15) two combinations.

The phase error bound can be obtained when the minimal value gap is *t*. Let $\Delta\phi_{\max} = \max(|\Delta\phi_1(x)|, |\Delta\phi_2(x)|)$, where $\Delta\phi_1(x)$ is the phase error of the wrapped phase map $\phi_1(x)$, $\Delta\phi_2(x)$ is the phase error of the wrapped phase map $\phi_2(x)$. From Statement 4 and using the similar analysis presented in [13], the phase error bound for two frequencies with the largest common factor t (t>1) can be obtained as follows:

$$0 \le \Delta\phi_{\max} < \frac{t\pi}{f_1 + f_2} \tag{22}$$

The above gives the upper bound of $\Delta\phi_{\max}$ with which the absolute phase maps can be correctly recovered. In other words, if $\Delta\phi_{\max}$ is given, we should select the two frequencies to meeting the following:

$$f_1 + f_2 < \frac{t\pi}{\Delta\phi_{\max}} \tag{23}$$

Compared with [13], the reliability of absolute phase maps can be significantly improved in terms of the phase error tolerance.

4. Experiments

In order to verify the performance of the proposed technique, we implemented two experiments. The aim of first experiment is to show that the proposed three-frequency method could recover the absolute phase of test object correctly. The aim of second experiment is to show the proposed three-frequency method could improve the reliability of the absolute phase recovered by two-frequency method. The camera in the experiments is DuncanTech MS3100 high resolution 3CCD camera, the projector is Hitachi CP-X260 Multimedia LCD Projector. The test object is a plaster hand, which is characterized by complex surface such as sharp changes and

discontinuities around fingers. Similar surfaces can be found in many engineering applications, thus it is used to demonstrate the effectiveness of proposed method. The length (along the finger direction) of the test object is 250mm, the width is 160mm, and the maximal height is 80mm.

In the first experiment, we project three fringe patterns at spatial frequencies $f_1 = 10$, $f_2 = 12$, $f_3 = 15$ onto the same plaster hand model. The two combinations for phase unwrapping are (10,15) and (12,15), the minimal value gap of $\frac{f_3\phi_1(x) - f_1\phi_3(x)}{2\pi}$ (10,15) is 5, the minimal value gap of $\frac{f_3\phi_2(x) - f_2\phi_3(x)}{2\pi}$ (12,15) is 3. The wrapped phase maps are obtained by six-step PSP (Phase Shifting Profilometry). The deformed fringe patterns are shown in Fig. 1 (a) - (c), the vertical (*y*-direction) resolution of pattern image is 1392, the horizontal (*x*-direction) is 1038. The capture field of camera is 464mm (*y*-direction) × 346mm (*x*-direction), so the periods of spatial frequencies $f_1 = 10$, $f_2 = 12$, $f_3 = 15$ are 346mm/10=34.6mm, 346mm/12=28.83mm, 346mm/15=23.09mm. These periods are achieved by controlling the projector pitches in our experiments.

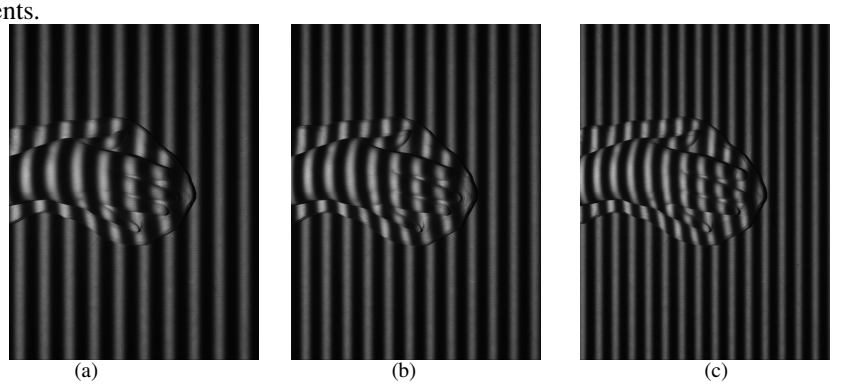

(a) (b) (c)

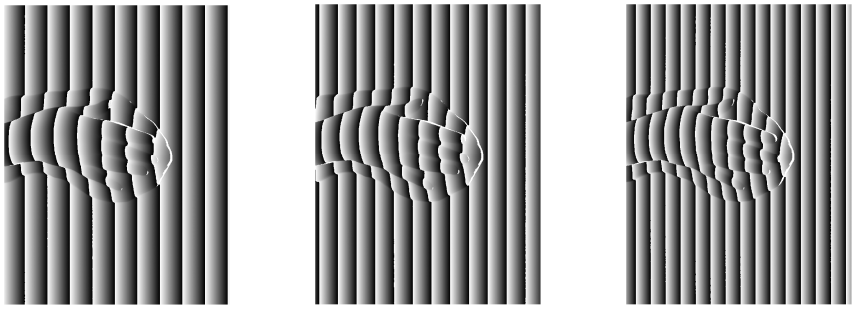

(d) (e) (f)

(g) (h) (i)

Fig. 1 Experiment results when $f_1 = 10$, $f_2 = 12$, $f_3 = 15$. (a)-(c) are the deformed fringe pattern on $f_1 = 10$, $f_2 = 12$, $f_3 = 15$ respectively; (d)-(f) are the wrapped phase maps on each frequency obtained by six-step PSP; (g)-(i) are the recovered absolute phase maps on each frequencies by (d)-(f).

To obtain the maximum absolute value of phase error in wrapped phase map, we compare the wrapped phase calculated by captured fringe images on reference plane (six-step phase shifting algorithm) with the ideal wrapped phase at $f_1 = 10$ generated by computer. The maximum absolute value of phase error in the wrapped phase in our system is 0.1387, the phase error is mainly resulted from the nonlinearity of the system. When the number of phase shifting is determined, the phase error is a periodic function of its corresponding actual phase [17, 18], so we can use this value to estimate the phase error for the fringes at different frequencies. Comparing with the phase error bound given by Eq. (22), we know that the maximum absolute value of phase error is smaller than the phase error bound, $0.1387 < 5\pi/(10+15) = \pi/5$ and $0.1387 < 3\pi/(12+15) = \pi/9$. In this case, the absolute phase maps should be recovered correctly and the results in Figure 1 (g)-(i) has shown the same. Figure 2 (a) are the sections $y = 800$ (pixel) on the absolute phase maps of three digital frequencies. Those absolute phases on section *y*=800 (pixel) are sampled from the absolute phase maps in Figure 1 (g)-(i), we mark the section *y*=800 of $f_1 = 10$ by a solid black line in Figure 2 (b), the position of the section is the same for other frequencies. The amplitudes of recovered absolute phases at different frequencies are consistent with the analytical conclusions given in [13].

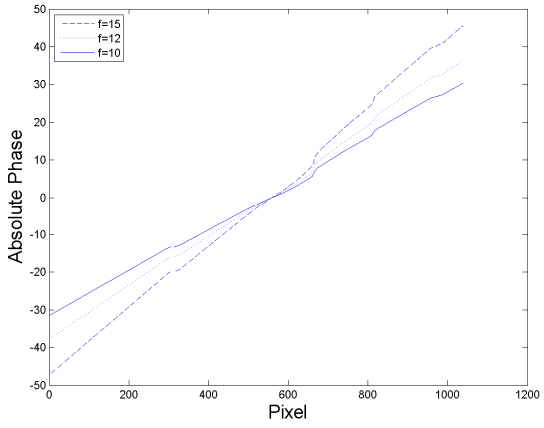

(a)

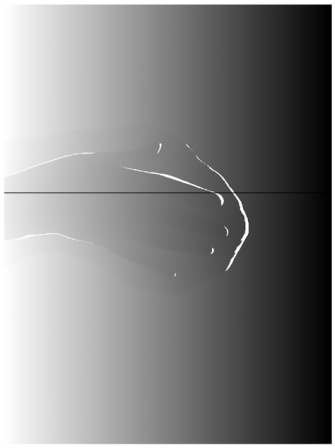

(b)

Fig. 2 Absolute phases on the section $y = 800$ (pixel) of three spatial frequencies (a) and position of section *y*=800 (b)

The second experiment aims to validate the increase of the value gap by the proposed frequency selection method in Section 3. The experiment firstly reconstructs the three-dimensional surface of an object (a hand) using the proposed three frequency technique where the three frequencies are selected as $f_1 = 8$, $f_2 = 12$, $f_3 = 15$, the two combinations for phase unwrapping are (8,12) and (12,15), the minimal value gap of $[f_2\phi_1(x) - f_1\phi_2(x)]/2\pi$ (8,12) is 4, the minimal value gap of $[f_3\phi_2(x) - f_2\phi_3(x)]/2\pi$ (12,15) is 3. The periods of different frequency fringes are also achieved by controlling the projector pitches.

The result of the 3D reconstruction is shown in Figure 3. Then we reconstruct the same object using the two frequency technique [12 ,13] where the two frequencies are 8 and 15, and the result is shown in Figure 4. The wrapped phase maps are all obtained by six-step PSP. The errors in Figure 4 do not belong to the invalid regions, the absolute phase in invalid regions are labeled as infinite (appeared as white region) in Figure 4.

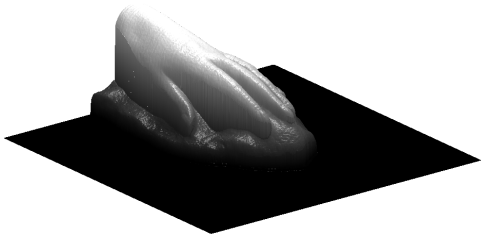

Fig. 3 Three-dimensional cloud reconstructed by three frequency technique at $f = 15$

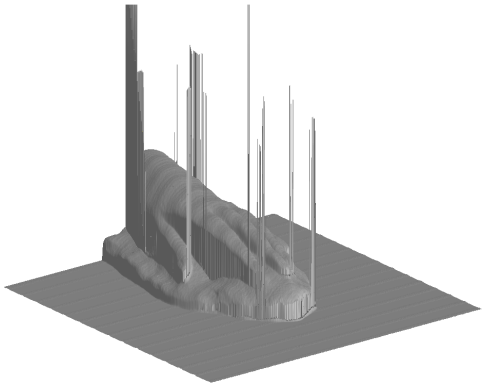

Fig. 4 Three-dimensional cloud reconstructed by two frequency technique at $f = 15$

Similar to experiment 1, the maximum absolute value of the phase error in wrapped phase maps is 0.1387, which is still smaller than the phase error bound $4\pi/(8+12) = \pi/5$ and $3\pi/(12+15) = \pi/9$ given by Equation (22). Hence the proposed method is able to recover the absolute phase, thus yielding correct 3D shape reconstruction as shown in Figure 3. However, for the two frequency method in [12, 13], although the maximum absolute value of the phase error in wrapped phase maps is still 0.1387, this value is larger than the phase error bound $0.1387 > \pi/(8+15) = \pi/23$ given in [13]. Hence mistakes are resulted for determining the fringe indices and errors can be observed in Figure 4 for the 3D reconstruction of the object. To evaluate the performance of three frequency technique and two frequency technique, we count the number of pixels with wrong fringe order recovered by those two techniques. In this experiment, the number of pixels with wrong fringe order in the absolute phase map recovered by two frequency technique at $f = 15$ is 227, in contrast, there is no pixel with wrong fringe order in the absolute phase map recovered by three frequency technique at $f = 15$. To compare the results in detail, we use the section y=565 to show the difference of the absolute phases recovered by those two techniques.

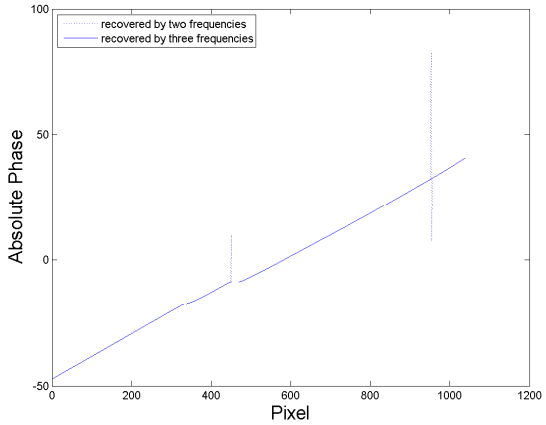

Fig. 5 Absolute phase recovered by two frequency technique and three frequency technique on section y=565 at $f = 15$

From Figure 5, we can see that the absolute phase recovered by two frequency technique overlaps with the absolute phase recovered by three frequency technique except few significant

errors, the errors are resulted from the wrong fringe orders [13]. These results show that the proposed method is better than the two-frequency one [12, 13] in terms of its anti-phase error capability.

5. Conclusion

This paper proposes a temporal phase unwrapping technique based on projection of three fringe patterns with different frequencies. A general rule is also presented for selecting the three frequencies with the aim to increase anti-phase error capability. It is shown by theoretical analysis and experiments that, under the same level of phase error, the proposed three frequency technique can provide a more reliable phase unwrapping result than the two frequency technique in [12, 13]. The proposed three frequency technique can be employed to acquire the three dimensional data accurately for the objects characterized by complex surface.

References and links

1. S. Zhang, X. Li and S. Yau, "Multilevel quality-guided phase unwrapping algorithm for real-time dimensional shape reconstruction," Appl. Opt. **46**, 50-57 (2007).
2. J. M. Huntley and H. O. Saldner, "Temporal phase-unwrapping algorithm for automated interferogram analysis," Appl. Opt. **32**, 3047-3052 (1993).
3. H. Zhao, W. Chen and Y. Tan, "Phase-unwrapping algorithm for the measurement of three-dimensional object shapes," Appl. Opt. **33**, 4497-4450 (1994).
4. H. J. Chen, J. Zhang, D. J. Lv and J. Fang, "3-D shape measurement by composite pattern projection and hybrid processing," Opt. Express **15**, 12318-12330 (2007).
5. J. Li, H. Su and X. Su, "Two-frequency grating used in phase-measuring profilometry," Appl. Opt. **36**, 277-280 (1997).
6. J. Li, L. G. Hassebrook and C. Guan, "Optimized two-frequency phase-measuring-profilometry light-sensor temporal-noise sensitivity," J. Opt. Soc. Am. A. **20**, 106-115 (2003).
7. K. Liu, Y. Wang, D. L. Lau, Q. Hao and L. G. Hassebrook, "Dual-frequency pattern scheme for high-speed 3-D shape measurement," Opt. Express **18**, 5229-5244 (2010).
8. J. M. Huntley and H. O. Saldner, "Error-reduction methods for shape measurement by temporal phase unwrapping," J. Opt. Soc. Am. A **14**, 3188-3196 (1997).
9. H. O. Saldner and J. M. Huntley, "Temporal phase unwrapping: application to surface profiling of discontinuous objects," Appl. Opt. **36**, 2770-2775 (1997).
10. S. Zhang, "Digital multiple-wavelength phase-shifting algorithm," Proc. SPIE **7432**, 74320N (2009).
11. S. Zhang, "Phase unwrapping error reduction framework for a multiple-wavelength phase-shifting algorithm," Opt. Eng. **48** (2009).
12. Y. Ding, J. Xi, Y. Yu and J. Chicharo, "Recovering the absolute phase maps of two fringe patterns with selected frequencies," Opt. Lett. **36**, 2518-2520 (2011).
13. Y. Ding, J. Xi, Y. Yu, W. Cheng, S. Wang, and J. Chicharo, "Frequency selection in absolute phase maps recovery with two frequency projection fringes," Opt. Express **20**, 13228-13251 (2012).
14. J. Zhong, M. Wang, "Phase unwrapping by a lookup table method: application to phase maps with singular points," Opt. Eng. **38**, 2075-2080 (1999).
15. J. Zhong, Y. Zhang, "Absolute phase-measurement technique based on number theory in multifrequency grating projection profilometry," Appl. Opt. **40**, 492-500 (2001).
16. J. Zhong, "Linear integer unconcerned phase-map profilometry by changing the projection angle of the grating," Opt. Eng. **40**, 1377-1382 (2001)
17. K. Liu, Y. Wang, D. L. Lau, Q. Hao and L. G Hassebrook, "Gamma model and its analysis for phase measuring profilometry," J. Opt. Soc. Am. A **27**, 553-563(2010).
18. B. Pan, Qian K., L. Huang, and A. Asundi, "Phase error analysis and compensation for nonsinusoidal waveforms in phase-shifting digital fringe projection profilometry," Opt. Lett., **34**, 416-418 (2009)